ASSESSMENT OF THE ORGANIZATION OF A TURBULENT SEPARATED AND REATTACHING FLOW BY MEASURING WALL PRESSURE FLUCTUATIONS

Woong Kang
Department of Mechanical Engineering,
Korea Advanced Institute of Science and Technology,
373-1, Gusong-dong, Yusong-gu, Daejon, 305-701, KOREA
gracekang@kaist.ac.kr

Hyung Jin Sung
Department of Mechanical Engineering,
Korea Advanced Institute of Science and Technology,
373-1, Gusong-dong, Yusong-gu, Daejon, 305-701, KOREA
hjsung@kaist.ac.kr

ABSTRACT

The effect of local forcing on the organization of a turbulent separated and reattaching flow was assessed by measuring wall pressure fluctuations. Multi-arrayed microphones were installed on the surface to measure the simultaneous spatial and temporal wall pressure fluctuations. Local forcing at the separation edge was applied to the separated flow over a backward-facing step through a thin slit. The organization of the separated and reattaching flow was found to be greatest at the effective forcing frequency. The flow structure was diagnosed by analyzing several characteristics of the wall pressure fluctuations: the wall pressure fluctuation coefficients, wall pressure spectrum, wavenumber-frequency spectrum, coherence, cross-correlation, and multi-resolution autocorrelations of pressure fluctuations using the maximum overlap discrete wavelet transform and continuous wavelet transform. Features indicative of the amalgamation of vortices under the local forcing were observed; this amalgamation process accounted for the observed reduction of the reattachment length. Examination of the wall pressure fluctuations revealed that introduction of local forcing enhanced flapping motion as well as the streamwise and spanwise dispersions of vortical structures.

INTRODUCTION

Numerous attempts have been made to control turbulent separated and reattaching flows. One approach that has received considerable attention is local forcing at the separation edge (Miau et al. 1991; Sigurdson 1995; Chun and Sung 1996; Kiya et al. 1997; Chun and Sung 1998; Yoshioka et al. 2001). Chun and Sung (1996) showed that applying local forcing at the effective forcing frequency maximized the organization of the turbulent separated and reattaching flow over a backward-facing step. To assess the flow organization, they made extensive measurements of various quantities, including mean and turbulent velocity quantities, reattachment length and velocity spectra. Such measurements of the entire flow structure are very time consuming. A simple and efficient alternative approach to assessing the organization of flow structure is to measure the wall pressure fluctuations on the surface. Such measurements can be used to probe the flow structure because wall pressure fluctuations are closely related to the vortical flow structures above the wall. Furthermore, wall pressure fluctuations are footprints of the vortices convecting over the wall (Kim et al. 2002).

Many studies of wall pressure fluctuations have been made to elucidate the unsteady behaviors of separated and reattching flows, for example flapping of the reattaching shear layer and shedding of large-scale vortical structures. Kiya and Sasaki (1983) examined the large-scale vortical structure in the reattaching zone through consideration of the cross-correlations between wall pressure fluctuations and velocity fluctuations. The large-scale vortical structure was educed by a conditional signal of wall pressure fluctuations (Kiya and Sasaki 1985). Farabee and Casarella (1986) measured the wall pressure spectra of separated flows using a single microphone. Subsequent to this, other workers have used multi-arrayed microphones to measure time-mean statistics (Lee and Sung 2002) and spatio-temporal characteristics (Lee and Sung 2002; Hudy et al. 2003). Recently, the interaction between the unsteady wake and turbulent separated and reattaching flow over a backward-facing step was examined by means of synchronized measurements of the streamwise and spanwise wall pressure fluctuations (Chun et al. 2003). In other work, conditional sampling in the spatial domain with a spatial box filtering of wall pressure fluctuations was adopted to extract the large-scale vortical structure under the influence of a periodic wake (Lee and Sung 2002). The main objective of the present study is to assess the organization of a turbulent separated and reattaching flow by measuring wall pressure fluctuations. The system chosen for study was that used previously by Chun and Sung (1996), namely a separated and reattaching flow with local forcing. This system was selected because the turbulent separated and reattaching flow is well organized by imposing local forcing at the effective forcing frequency. Multi-arrayed microphones were installed in the bottom wall surface of the flow over a backward-facing step. The flow forcing condition was the same as that used by Chun and Sung (1996). Synchronized measurements of the wall pressure fluctuations in both the streamwise and spanwise directions were performed using the multi-arrayed

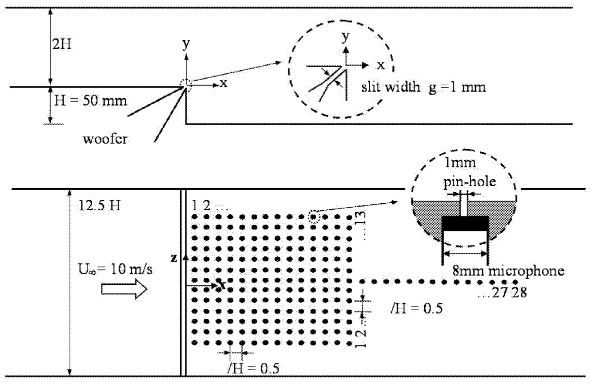

Figure 1: Experimental setup of backward-facing step with a speaker and arrangement of multi-arrayed microphones.

microphones. The wall pressure fluctuations with and without local forcing were compared. The flow organization was examined in terms of the wall pressure spectrum, pressure fluctuation coefficients, auto- and cross-correlations, and the wavenumber-frequency spectrum. The temporal and spatial characteristics of the vortical structures were analyzed using the maximum overlap discrete wavelet transform (MODWT) and continuous wavelet transform (CWT). At the effective forcing frequency, amalgamation of the spanwise vortices occurred to the greatest extent, leading to a maximum reduction of the reattachment length.

EXPERIMENTAL APPARATUS AND PROCEDURE

Experiments were performed in a subsonic open-circuit wind tunnel. Details regarding the experimental apparatus and the acoustic local forcing can be found in Chun and Sung (1996) and Lee and Sung (2002). Special attention was given to minimizing tunnel floor vibration caused by the woofer speaker used to drive the local forcing. The characteristic length of the backward-facing step was defined as the step height, H=50mm. The aspect ratio AR based on H was 12.5 to ensure that the flow was two-dimensional (Brederode and Bradshaw 1978). In the present study, the free-stream flow speed used was 10 m/s, resulting in a Reynolds number of 33,000 based on the step height H. The boundary layer thickness δ , displacement thickness δ^* , and momentum thickness θ of the inlet boundary layer at x/H=-0.02 were 20.0 mm, 3.1 mm and 2.3 mm, respectively.

A total of 182 ICP-type microphones (TMS060A, Soritel Inc., Korea) were used; they were installed on the bottom surface of the expanded duct as shown in figure 1. The microphones were installed in the $y = 0$ plane at uniform intervals of 0.5H ($1.25 \leq x/H \leq 8.75$, $-3.0 \leq z/H \leq 3.0$). Synchronized measurements of wall pressure fluctuations with 14 microphones in the streamwise direction and 12 microphones in the spanwise direction were carried out. To increase the spatial and frequency resolution of each microphone, a pinhole of diameter 1 mm and an installation cavity of diameter 8 mm were drilled concentrically on the bottom plate (Chun et al. 2003). Two 16-channel differential amplifiers (PCB 513, The Modal Shop Inc.) were used to provide excitation power for the microphone, as well as to amplify the fluctuating voltage signals. Each microphone was calibrated against a 0.5-inch B&K 4133 microphone. To exclude the data scatter associated with the uncertainty of the microphone calibration procedure (Hudy et al. 2003), the wall pressure fluctuation coefficients and wall pressure spectra along the streamwise direction were obtained by sequential measurements using a single microphone. Simultaneous acquisition of the wall pressure fluctuation signals from the 28 microphones was performed using LabVIEW software and a 64-channel A/D board (NI6110, National Instruments Inc.). A total of 409,600 time series data were acquired for each microphone at a sampling frequency of 7812.5 Hz.

Preliminary velocity measurements were carried out using a constant-temperature anemometer (IFA 300). The forcing amplitude was calibrated using a single-wire probe (TSI 1260) with a 5μm tungsten wire. The sampling frequency was fixed at 5kHz. A split-film probe (TSI 1288) was used to measure the reattachment length (x_R), defined as the point where the forward-flow time fraction (γ_p) in the vicinity of the wall ($y/H = 0.01$) is equal to $\gamma_p = 0.5$. To resolve the time-mean reattachment length, the sampling frequency was fixed at 200Hz, and a total of 60,000 data were obtained, indicating that around 1,500 flapping motions ($St = 0.025$) were encompassed in the measurement.

In the present study, care was exercised to clarify the spatio-temporal characteristics of the wall pressure fluctuations. To this end, three forcing frequencies, $St_f = 0, 0.275$ and 1.5, were chosen for comparison. The reattachment length of the separated and reattaching flow was reduced from $x_R/H = 7.75$ at $St_f = 0$ to $x_R/H = 5.65$ at $St_f = 0.275$, and increased to $x_R/H = 8.02$ at $St_f = 1.5$. These results are consistent with those of Chun and Sung (1996). Chun and Sung (1996) defined the forcing amplitude A_0 as the momentum change between the unforced flow and the forced flow in the initial boundary layer. However, this definition is not useful for numerical simulation applications. A simple definition, $A_0 = v_{rms}/U_\infty$, is better for numerical simulations, where v_{rms} is the root-mean-square of the total velocity fluctuations at the slit edge ($x/H = -0.01, y/H = 0$). It is found that the previous forcing amplitude of Chun and Sung, $A_0 = 0.03$, corresponds to $v_{rms}/U_\infty = 0.6$. The wall pressure fluctuations in the

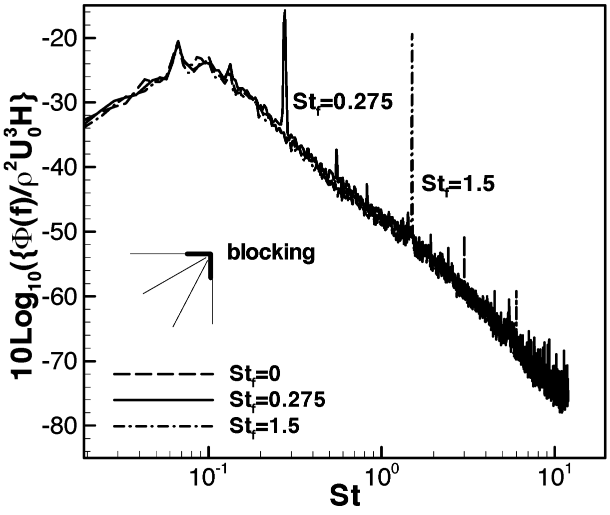

Figure 2: Wall-pressure spectrum influenced by background sound of speaker at $x/H = 7.75$.

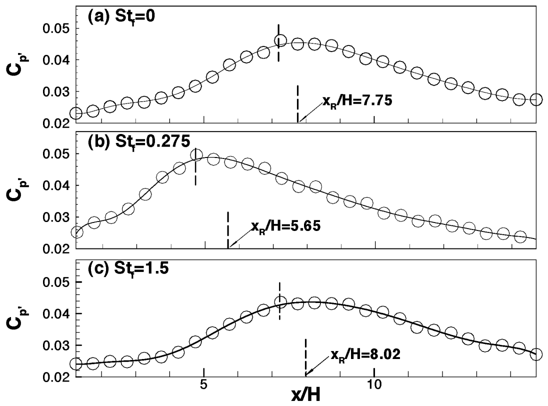

Figure 3: Wall-pressure fluctuation coefficient a) $St_f = 0$ b) $St_f = 0.275$ c) $St_f = 1.5$.

time, frequency and wavenumber domains were analyzed in terms of the wall pressure fluctuation coefficients, autospectrum, coherence, wavenumber-frequency spectrum, and both the MODWT and CWT (Percival and Walden 2000).

EXPERIMENTAL RESULTS AND DISCUSSION

When the local forcing experiments were performed in the present work, a severe speaker sound at higher forcing frequency was generated that could potentially influence the microphones installed on the surface as a background noise. Hence, prior to the main experiments, we examined the influence of this background noise. To this end, the jet slit was blocked and no flow excitation was applied through the thin slit. The wall pressure spectrum at $x/H = 7.75$ was measured for three forcing frequencies, St_f=0, 0.275 and 1.5; the resulting spectra are shown in figure 3. Close inspection of figure 3 reveals a very slight difference in the lower frequency region (St≤0.2). The results indicate that the background noise from the speaker has no significant effect for the three forcing cases, although distinctive peaks were found at the forcing frequencies and their harmonics. As expected, the shedding of large-scale vortices and flapping of the reattaching shear layer were observed in the lower frequency region. This suggests that the background noise has a negligible effect on the two main types of unsteady behavior.

To clarify the global characteristics of the separated and reattaching shear layer, streamwise distributions of the rms pressure fluctuations, $C_{p'}$, normalized by the inflow dynamic pressure, q, were determined (figure 4) (Lee and Sung 2001, 2002; Chun et al. 2003). For the no forcing case (St_f =0), increases along the streamwise direction in the range $0 \leq x/H \leq 7.25$, and then decreases on moving further downstream ($x/H \leq 7.25$). The maximum $C_{p'}$ occurs slightly upstream (∼1H) of the time-mean reattachment point, in agreement with previous results (Lee and Sung 2001). When the forcing is applied at St_f =0.275, the position of the maximum $C_{p'}$ moves upstream by 2.5H. The $C_{p'}$ distribution at St_f=1.5 is similar to that at St_f=0. The correlation between x_R and $C_{p'}$ indicates that x_R can be predicted by measuring the location of the maximum $C_{p'}$(1H downstream), without direct measurement of x_R.

The influence of local forcing on the spatial development of vortical structure was obtained by measuring the wall pressure spectrum along the streamwise direction. Figure 4 shows the wall pressure spectra at four positions (x/H=1.25, 4.25, 5.75 and 7.75) for the three forcing frequencies, St_f =0, 0.275 and 1.5. Near the separation edge(x/H = 1.25), three characteristic frequencies are detected in figure 4a) at St = 0.02, 0.07, and 0.13. The feature at St = 0.02 corresponds to the flapping frequency, where the normalized frequency fx_R/U_0=0.16 coincides with the value of Mabey (1972). The shedding frequency is at St = 0.07, which is close to the values of St = 0.068 and 0.067 reported by Eaton and Johnston (1980) and Lee and Sung (2002) respectively. The merging frequency is detected at St = 0.13, which corresponds to the first subharmonics of the forcing frequency (St_f = 0.275). This suggests that a large-scale vortex amalgamation takes place in the separated shear layer due to the local forcing. This vortex merging causes the increase in turbulence intensities so that the overall turbulence levels are significantly enhanced. When the local forcing is applied at St_f =0.275, flapping is significantly enhanced. It is interesting to note that forcing at the high frequency of St_f =1.5 has little effect on the wall pressure fluctuations. For both forcing cases (St_f =0.275 and 1.5), the higher frequency region of the spectrum is contaminated by the forcing frequency and its harmonics. At x/H = 4.25 (figure 4b)), forcing at St_f = 0.275 causes a large upward shift of the spectrum with respect to the St_f = 0 spectrum, whereas forcing at St_f = 1.5 leads to a slight downward shift. The strengths of the flapping, shedding and merging frequencies are significantly enhanced by forcing at St_f = 0.275, which gives broadband rise in the spectrum. The enhancement of flapping motion is closely related to the removal of corner flow by the local forcing (Chun and Sung 1996). The merging frequency at St = 0.13 appears to be strong as compared with other local forcings. This promotes the amalgamation of spanwise vortices, leading to a large degree of entrainment close to the separation edge, which pushes the time-averaged streamlines toward the wall (Chun and Sung 1996). The slight downward shift of the spectrum at St_f = 1.5 with respect to the St_f = 0 spectrum demonstrates that the quasi-deterministic

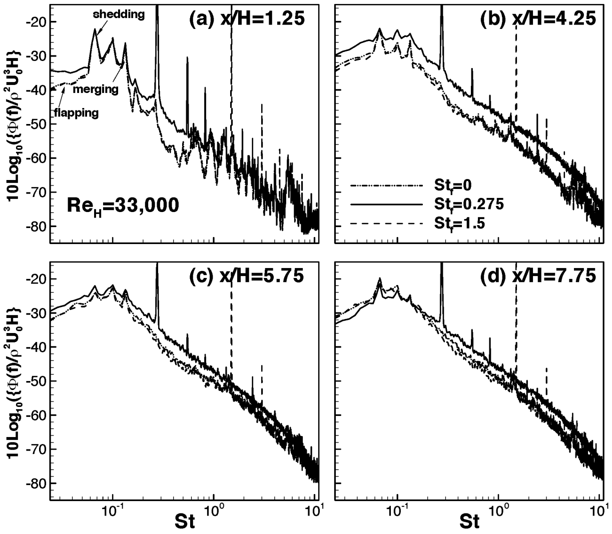

Figure 4: Wall-pressure spectrum a) $x/H = 1/25$ b) $x/H = 5.25$ c) $x/H = 5.75$ d) $x/H = 10.25$.

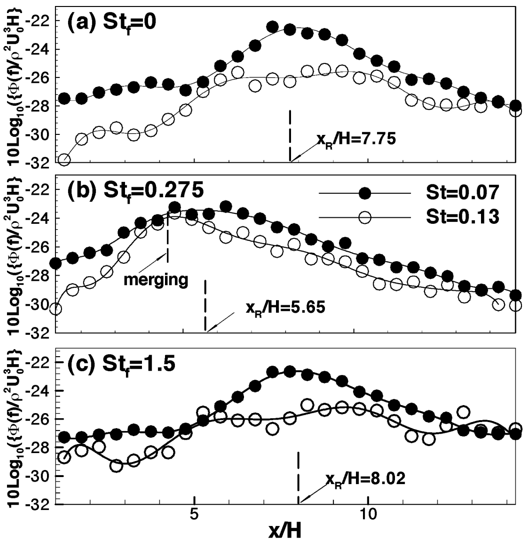

Figure 5: Spatial development of wall-pressure spectrum at $St = 0.07$ and $St = 0.13$ a) $St_f = 0$ b) $St_f = 0.275$ c) $St_f = 1.5$.

coherent vortex structure is attenuated at higher forcing frequencies. As shown in figure 5c), the intensity of shedding is enhanced for three cases. Recall that the reattachment length at $St_f = 0.275$ ($x_R/H = 5.65$) is close to the location at which the spectra shown in figure 5c) were recorded ($x/H = 5.75$). Thus, as the flow goes downstream from $x/H = 5.75$, the vortical structure in the flow subjected to forcing at $St_f = 0.275$ decays, whereas the vortical structure in the $St_f = 0$ system begins to develop until reattachment at $x/H = 7.75$. At $x/H = 7.75$ (figure 4d)), the $St_f = 0.275$ spectrum is attenuated at low frequencies such that the spectrum falls below the $St_f = 0$ spectrum in that region.

Further comparison of the variations in the spatial strength of the vortical structure at the shedding and merging frequencies is made for the three forcing cases. Two frequencies are chosen, namely the shedding frequency and the merging frequency ($St = 0.07$ and $St = 0.13$ respectively). The magnitude of the wall pressure spectrum at each of these frequencies is plotted as a function of x/H in figure 5 for the three forcing cases. For forcing at $St_f = 0.275$, the magnitude of the spectrum at $St = 0.13$ rapidly increases near the separation edge up to a maximum value near $x/H = 4.25$ and then quickly decays on moving further downstream. This trend is consistent with a rapid amalgamation of spanwise vortices. Recall that $C_{p'}$ near the separation edge rapidly increases at $St_f = 0.275$. This is attributed to the dominance of the energetic shedding and merging motions. For the $St_f = 0$ and $St_f = 1.5$ systems, the magnitudes of their spectra at $St = 0.13$ slowly increase up to a maximum near $x/H = 5.75$, after which flat plateaus centered at $x/H = 7.75$ are formed. As mentioned above, the wall pressure fluctuations in the $St_f = 0$ system resemble those observed at $St_f = 1.5$, although the effect of $St_f = 0.275$ is apparent. Accordingly, two forcing cases, $St_f = 0$ and $St_f = 0.275$, are chosen for further discussion.

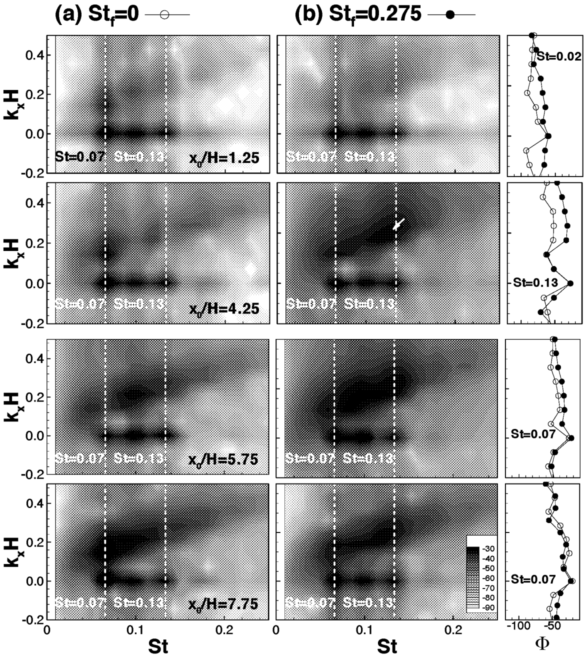

Figure 6: Streamwise wavenumber-frequency spectrum a) $St_f = 0.07$ and b) $St_f = 0.275$.

To assess the organization of the flow structure induced by local forcing, we now consider the wall pressure fluctuations in terms of the wavenumber-frequency spectra. The streamwise wavenumber-frequency spectrum $\Phi_{pp}(k_x, f; x_0)$ is obtained by Fourier transforming the streamwise cross spectrum $\Phi_{pp}(k_x, f; x_0)$ with respect to ξ. Figure 6 shows the streamwise wavenumber-frequency spectra for the $St_f = 0$ and $St_f = 0.275$ systems. For comparison, this figure also shows the spectra at three fixed frequencies, $St = 0.02, 0.07$ and 0.13. The streamwise wavenumber-frequency spectrum exhibits two distinctive convective ridges near the separation edge ($x/H = 1.25$), in good agreement with previous reports (Lee and Sung 2002; Hudy et al. 2003). These ridges, one slanted and the other horizontal (i.e., along k_x =0), are signatures of the shedding of large-scale vortices and of flapping of the reattaching shear layer, respectively. From the angle of the slanted ridge, the convection velocity of the large-scale vortices was calculated as U_c/U_∞ =0.56. Introduction of local forcing at $St_f = 0.275$ has no clear effect on the spectra recorded near the separation edge. However, when the reference point moves to $x/H = 4.25$, local forcing at $St_f = 0.275$ globally increases the strength of the slanted ridge, and induces a discrete bubble-like area at $St = 0.13$. These features are indicative of a strong amalgamation of the spanwise vortices. Local forcing at $St_f = 0.275$ enlarges the frequency content of the convective ridge to include high frequencies. The dispersion of the large-strength area along $St = 0.07$ indicates an expansion of the area influenced by the large-scale vortical structure. Such dispersion of the vortical structure due to the local forcing is clear up to $x/H = 5.75$. In fact, the extension of the frequency contents of the convection ridge due to the local forcing is not attenuated even at $x/H = 7.75$; however, at this downstream location the dispersion along $St = 0.07$ is similar for the two forcing cases. For the shedding vortical structure at $St = 0.07$, the strength at St_f=0.275 and $x/H = 5.75$ is even weaker than the strength at St_f =0 and $x/H = 7.75$. These characteristics of the streamwise wavenumber-frequency spectra are in good agreement with the trends in the wall pressure

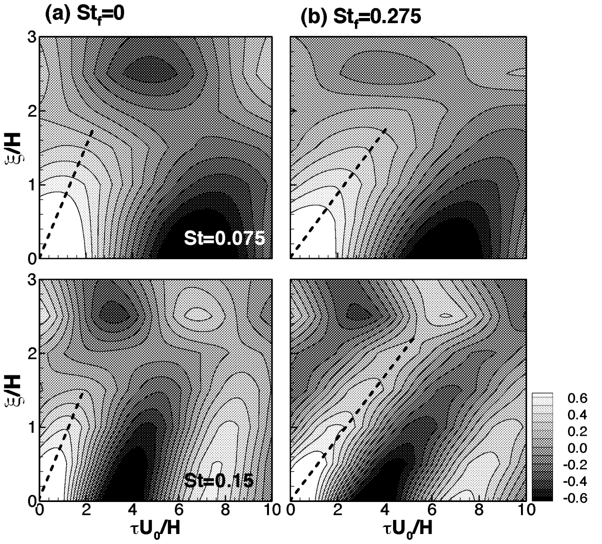

Figure 7: Streamwise cross-correlation of MOWDT transformed wall pressure flucutations at a) $St_f = 0.07$ and b) $St_f = 0.275$.

spectra in figure 4 and 5.

The spatio-temporal behavior of the process of spanwise vortex amalgamation was scrutinized through a time-dependent analysis of these vortical structures. By transforming the synchronized streamwise wall pressure fluctuations using the MODWT, the vortical structures centered at $St = 0.07$ and $St = 0.13$ are elucidated by cross-correlation of the extracted pressure signals. The cross-correlation is defined as

$$\rho_{pp}(\xi, \tau; x_0) = \frac{< p'_f(x_0, z_0, t) p'_f(x_0 + \xi, t + \tau) >}{< p'_f(x_0, t) p'_f(x_0, t) >} \qquad (1)$$

where $p'_f$is reconstructed by the inverse MODWT of the original pressure signals p' at the central frequency f. As shown in figure 7, local forcing causes the regions of large strength (indicated by dashed lines) to extend downstream. This is consistent with the enhanced dispersion of shedding and the amalgamation of spanwise vortices observed in the streamwise wavenumber-frequency spectra (figure 6). Moreover, the convection velocities of both the regular large-scale vortical structure and the amalgamation of spanwise vortices are slightly decreased by the local forcing. As discussed above, the discrete wavelet transformation of wall pressure fluctuations shows the intermittent scale-resolved vortical structures. However, the intermittent behaviors between $St = 0.13$ and $St = 0.275$ are not clearly detected due to the insufficient frequency resolution of discrete wavelet transformation, in which the central frequencies for each scale are approximated by half-band filters (Percival and Walden 2000). To overcome this problem, continuous wavelet transformation of the wall pressure fluctuations is employed to extract vortical structures with high frequency resolution. The continuous wavelet transform coefficient of time-series data can be defined as

$$w(b, a) = \frac{1}{a} \int_{-\infty}^{\infty} p'(t) \Psi(\frac{(t - b)}{a}) dt \qquad (2)$$

where a is the timescale dilation parameter and b is the time transition parameter. Parameters a and f are related by the conversion formula f=$\sqrt{2.5}/2\pi$a. The Mexican hat wavelet $\Psi(t) = (1 - t^2)exp(-\frac{1}{2}t^2)$ is used, which is known to be effective in resolving high amplitude peaks. To clarify the intermittent vortical structures with high frequency resolution, the autocorrelation of the CWT coefficients was analyzed. The wavelet auto-correlation function $wc(a, \tau)$ is defined as

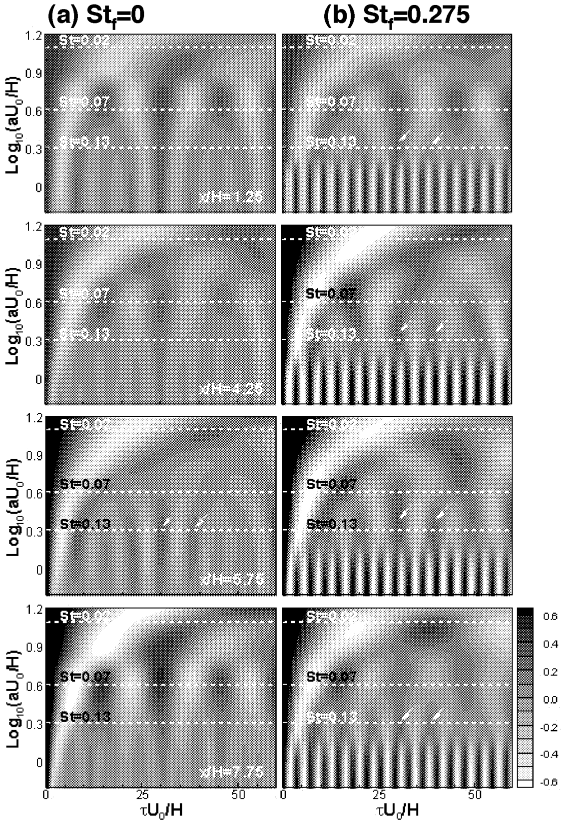

Figure 8: Auto-correlation of CWT coefficients of wall-pressure fluctuations a) $St_f = 0$ and b) $St_f = 0.275$.

$$wc(a, \tau) = \frac{w(b, a) w(b + \tau, a) >}{< w(b, a) w(b, a) >} \qquad (3)$$

where is the time delay of wavelet coefficients in the wavelet space. Figure 13 shows the auto-correlation of the CWT coefficients at $St_f = 0$ and $St_f = 0.275$. The main feature of interest in these plots is the interaction between the amalgamation of spanwise vortices and the forcing frequency. In the absence of forcing, areas of large strength (denoted by arrows) are observed at $x/H = 5.75$, indicating the quasi-deterministic appearance of the amalgamation of spanwise vortices, but these areas are indistinct at the upstream positions of $x/H = 1.25$ and 4.25. For $St_f = 0.275$, similar structures which are induced by two neighboring forcings at $St = 0.275$ are clearly exemplified at $x/H = 4.25$. Signatures of the strong amalgamation of spanwise vortices are clearly observed near the separation edge ($x/H = 1.25$) and at the downstream positions of $x/H = 5.75$ and 7.75.

CONCLUSIONS

The present study has shown that the organization of turbulent separated and reattaching flows can be efficiently delineated by examining the wall pressure fluctuations. In this work, the structure of the flow over a backward facing step was elucidated for three forcing cases ($St_f = 0, 0.275$ and 1.5) by carrying out measurements of the wall pressure fluctuations using multi-arrayed microphones rather than by direct measurement of the flow structure. The influence of local forcing was systematically analyzed in terms of the wall pressure fluctuation coefficients, wall pressure spectrum, cross-correlation, wavenumber-frequency spectrum and wavelet transforms. Introduction of forcing at $St_f = 0.275$ induced a large upstream shift of the wall pressure fluctuation coefficient, indicative of a reduction of the reattachment length. In addition, imposition of local forcing was shown to enhance the streamwise and spanwise dispersions of the vortical structures at $St = 0.07$ (the shedding of large-scale vortical structures) and $St = 0.13$ (the amalgamation of spanwise vortices). The amalgamation of spanwise vortices at $St_f = 0.275$ was clarified by examination of the wall pressure spectrum, as well as the multi-resolution auto-correlation of wall pressure fluctuations using the maximum overlap discrete wavelet transform and continuous wavelet transform. The intermittent amalgamation of spanwise vortices at $St = 0.13$ was the source of the reduction of the reattachment length. Additional enhancement of the flapping motion induced by local forcing was elucidated by use of the maximum overlap discrete wavelet transform.

REFERENCES

Brederode, V., and Bradshaw, P., 1978, "Influence of the side walls on the turbulent center-plane boundary-layer in a square duct", *Journal of Fluids Engineering*, Vol. 100, pp. 91-96.

Chun, K.B., and Sung, H.J., 1996, "Control of turbulent separated flow over a backward-facing step by local forcing", *Experiments in Fluids*, Vol. 21, pp. 417-426.

Chun, K.B., and Sung, H.J.,1998, "Visualization of locally-forced separated flow over a backward-facing step", *Experiments in Fluids*, Vol. 25, pp. 133-142.

Chun, S., Liu, Y.Z., and Sung H.J., 2004. "Wall pressure fluctuations of a turbulent separated and reattaching flow affected by an unsteady wake", *Experiments in Fluids*, Vol. 37, No. 4, pp. 531-546.

Eaton, J.K., and Johnston, J.P., 1981, "A review of research on subsonic turbulent flow reattachment", *AIAA Journal*, Vol. 19, pp. 1093-1100.

Farabee, T.M., and Casarella, M.J., 1986, "Measurements of fluctuating wall pressure for separated/reattached boundary layer flows", *Journal of Vibration, Acoustics, Stress Reliability in Design*, Vol. 108, pp. 301-307.

Hudy, L.M., Naguib, A.M., and Humphreys, W.M., 2003, "Wall pressure-array measurements beneath a separating/reattaching flow region", *Physics of Fluids*, Vol. 15, pp. 706-717.

Kim, J., Choi, J.I., and Sung, H.J., 2002, 'Relationship between wall pressure fluctuations and streamwise vortices in a turbulent boundary layer", *Physics of Fluids*, Vol. 14, pp. 898-901.

Kiya, M., and Sasaki, K., 1983, "Structure of a turbulent separation bubble", *Journal of Fluid Mechanics*, Vol. 137, pp. 83-113.

Kiya, M., and Sasaki, K., 1985, "Structure of large-scale vortices and unsteady reverse flow in the reattaching zone of a turbulent separation bubble", *Journal of Fluid Mechanics*, Vol. 154, pp. 463-491.

Kiya, M.,Shimizu, and M., Mochizuki, O., 1997, "Sinusoidal forcing of a turbulent separation bubble", *Journal of Fluid Mechanics*, Vol. 342, pp.119-139.

Kobashi, Y., 1986, "Wall pressure and its relation to turbulent structure of a boundary layer", *Experiments in Fluids*, Vol. 4, pp. 49-55.

Lee, I., and Sung, H.J., 2002, "Multiple-arrayed pressure measurement for investigation of the unsteady flow structure of a reattaching shear layer", *Journal of Fluid Mechanics*, Vol. 463, pp. 377-402.

Lee, I., Ahn, S.K., and Sung, H.J., 2004, "Three-Dimensional Coherent Structure in a Separated and Reattaching Flow over a Backward-Facing Step" *Experiments in Fluids*, Vol. 36, No. 3, pp.373-383.

Li, H., 1998, "Identification of coherence structure in turbulent shear flow with wavelet correlation analysis", *Journal of Fluids Engineering*, Vol. 120, pp. 778-785.

Miau, J.J., Lee, K.C., Chen, M.H., and Chou, K.C., 1991, "Control of separated flow by a two-dimensional oscillatory plate", *AIAA Journal*, Vol. 29, pp. 1140-1148.

Percival, D.B., and Walden, A.T., 2000, "Wavelet methods for time series analysis", Cambridge University Press.

Sigurdson, L.W., 1995, "The structure and control of a turbulent reattaching flow", *Journal of Fluid Mechanics*, Vol. 298, pp. 139-165.

Yoshioka, S., Obi, S., and Masuda, S., 2001, "Turbulence statistics of periodically perturbed separated flow over a backward-facing step", *International Journal of Heat and Fluid Flow*, Vol. 22, pp. 393-401.

Yoshioka, S., Obi, S., and Masuda, S., 2001, "Organized vortex motion in periodically perturbed turbulent separated flow over a backward-facing step", *International Journal of Heat and Fluid Flow*, Vol. 22, pp. 301-307.